Engine Speed Based Estimation of the Indicated Engine Torque

Master's thesis
performed at **Vehicular Systems**

by
Magnus Hellström

Reg nr: LiTH-ISY-EX-3569-2005

16th February 2005

Engine Speed Based Estimation of the Indicated Engine Torque

Master's thesis

performed at **Vehicular Systems**,
Dept. of Electrical Engineering
at **Linköpings universitet**

by **Magnus Hellström**

Reg nr: LiTH-ISY-EX-3569-2005

Supervisor: **Zandra Jansson**
  DaimlerChrysler AG
Per Andersson
  Linköpings universitet
Per Öberg
  Linköpings universitet

Examiner: **Associate Professor Lars Eriksson**
  Linköpings universitet

Linköping, 16th February 2005

Titel	Varvtalsbaserad estimering av indikerat motormoment
Title	Engine Speed Based Estimation of the Indicated Engine Torque
Författare Author	Magnus Hellström

Sammanfattning
Abstract

The aim of this master's thesis is to implement and evaluate a method for estimating the indicated engine torque. The method is developed by IAV GmbH, Fraunhofer-Institut and Audi AG. The determination of the indicated torque is based on high resolution engine speed measurements. The engine speed is measured with a hall sensor, which receives the signal from the transmitterwheel mounted on the crankshaft. A transmitterwheel compensation is done to compensate for the partition defects that arises in the production and thus enable a more precise calculation of the angular velocity. The crankshaft angle, angular velocity and angular acceleration are estimated and the help variable effective torque is calculated using these signals as input. Through a relationship between effective torque and the indicated pressure the indicated pressure is extracted from a map. The indicated torque is then calculated from the pressure.

The method is validated with data from an engine test bed. Because of the low obtainable sample rate at the test bed, 4MHz, quantisation errors arises at engine speeds over 1000 rpm. Therefore the model is validated for low engine speeds and the result is promising.

Nyckelord Keywords	Indicated torque, indicated pressure, finite automaton, transmitterwheel error, engine speed estimation

Abstract

The aim of this master's thesis is to implement and evaluate a method for estimating the indicated engine torque. The method is developed by IAV GmbH, Fraunhofer-Institut and Audi AG. The determination of the indicated torque is based on high resolution engine speed measurements. The engine speed is measured with a hall sensor, which receives the signal from the transmitterwheel mounted on the crankshaft. A transmitterwheel compensation is done to compensate for the partition defects that arises in the production and thus enable a more precise calculation of the angular velocity. The crankshaft angle, angular velocity and angular acceleration are estimated and the help variable effective torque is calculated using these signals as input. Through a relationship between effective torque and the indicated pressure the indicated pressure is extracted from a map. The indicated torque is then calculated from the pressure.

The method is validated with data from an engine test bed. Because of the low obtainable sample rate at the test bed, 4MHz, quantisation errors arises at engine speeds over 1000 rpm. Therefore the model is validated for low engine speeds and the result is promising.

Keywords: Indicated torque, indicated pressure, finite automaton, transmitterwheel error, engine speed estimation

Thesis Outline

Outline of the master's thesis.

Chapter 1 Introduction: A short introduction to the problem in objective.

Chapter 2 System Description: The parts of the engine that are of concern in this thesis are presented. A brief introduction to how a 4-stroke engine works over one cycle is given.

Chapter 3 Indicated Torque Modeling: The model approach is presented.

Chapter 4 Alternating Gas Torque Calculation: The equations for calculating the gas torque for a one cylinder engine are deduced and then expanded to a six cylinder engine.

Chapter 5 Manifold Pressure Dependence: A method to compensate for the higher gas torque which occurs for turbocharged engines.

Chapter 6 Transmitterwheel error compensation: A method to compensate for production errors on the transmitterwheel is presented.

Chapter 7 Cycle Duration Measurements: In this chapter different ways to measure and estimate the crank angle, angular velocity and angular acceleration, are discussed. These are the signals needed to calculate the alternating gas torque in Chapter 4.

Chapter 8 Measurements in an Engine Test Bed and in Vehicle This chapter presents the measurements done to get the validation data.

Chapter 9 Validation and Results: Validation and results are presented.

Chapter 10 Conclusions: The conclusions drawn from this master thesis are presented and discussed.

Chapter 11 Future Work: What can be done to improve and develop the model and its results are discussed.

Acknowledgment

Contents

Chapter 1

Introduction

The engine torque signal is a very important signal for powertrain control. The torque is nowadays calculated in the control unit of the vehicles, but the calculation does not always give an accurate result and a precise engine torque signal is desirable. If a more precise engine torque signal could be generated the car could be driven closer to optimum, with lower fuel consumption and better comfort as merits. The best way to achieve such a precise signal would of course be to measure the torque and thereby getting an accurate estimate. However, due to cost and integration complexity it is not profitable to use torque sensors in series production. Since an engine torque sensor is not an option, new models for torque estimation are developed and tested. The engine torque is affected by a lot of different sources such as fuel injection, air quantity, oil temperature, the temperature of the gear oil and so on. It is impossible to consider all interacting sources when building a model, so there will always be a difference between model and reality which can lead to deviations between the torque the engine provides and the estimated one.

Unlike torque sensors, the existing engine speed sensors are relatively cheap and accurate and it would be sensible to somehow use this information instead. The main topic of this master's thesis is the implementation and testing of the accuracy and feasibility of a new engine torque model, developed by IAV GmbH, Frauenhofer-Institut and Audi AG, which uses the signal from the engine speed sensor as input. The model is based on the determination of the crankshaft position which is used for estimation of the indicated pressure. The indicated torque is then calculated from the pressure.

1.1 Objective

The objectiv of this master thesis is to implement and evaluate a method to estimate the indicated engine torque developed by IAV GmbH, Frauenhofer-

Institut and Audi AG. The method is implemented as a model in Matlab/Simulink, with compensation for the transmitterwheel error. The model is to be tested and validated with data from an engine test bed.

Chapter 2

System Description

In this master's thesis a map based model which uses the engine speed signal as input to estimate the indicated torque is investigated. The indicated torque is the torque generated in the cylinders and acting on the crankshaft without friction.

This section gives an overview of the engine system producing the torque. The engine system considered here consists of a hall sensor, the crank shaft, a transmitterwheel, pistons and piston rods, as seen in Figure 2.1.
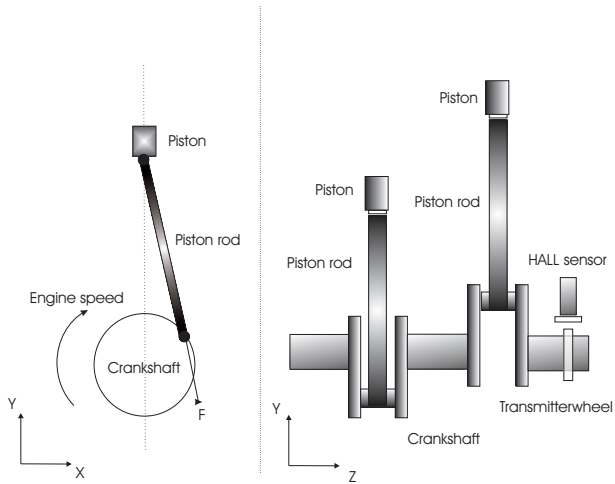

Figure 2.1: The engine system, seen from two angles of perspective

The engine operates in four strokes. In the first air is inhaled as the piston moves down, in the second the air is compressed as the piston moves up. At the peak of compression the fuel is injected and ignited. The ignition sets energy free and increases the gas pressure in the cylinder that forces the piston to move down. Every time when the engine ignites there is a peak in the engine speed, if it is a six cylinder engine there are six peaks in the engine speed per two revolutions. The forth stroke is when the piston moves up and ejects the exhausts. The work delivered to the piston over the entire four stroke cycle, per unit displaced volume, is called the net mean effective indicated pressure ($imep$). It is an efficiency norm that can be used to compare engines with different cylinder volumes, see [2]. The force that works on the piston is transmitted to the crankshaft through the piston rod. The crankshaft is put into rotation by the applied force and the torque on the powertrain is used to put the wheels in motion.

A combustion cycle consists of two crankshaft revolutions. A sensors on the camshaft is used to decide if it is the first or second revolution. To be able to tell in which part of the cycle the engine is at the moment the crankshaft position must be known. A transmitterwheel with 60 minus 2 teeth, where the two teeth left out are for synchronization, is assembled on the crankshaft to enable position determination. A hall sensor receives the signal from the transmitter wheel. The signal is used to detect when a new tooth occurs at the hall sensor, which is equal to an edge in the hall sensor output. Every edge implies an increase of six degrees except the one after the two teeth gap which implies a 18 degree change.

With the edges detected and hence the position determined, the $imep$ can be found through estimations, calculations and maps.

Chapter 3

Indicated Torque Modeling

The model approach is presented in this chapter. The basic principle is an accurate determination of the angular velocity and the crank shaft position. The model approach is summarized in Figure 3.1, p_{boost} is the boost pressure.
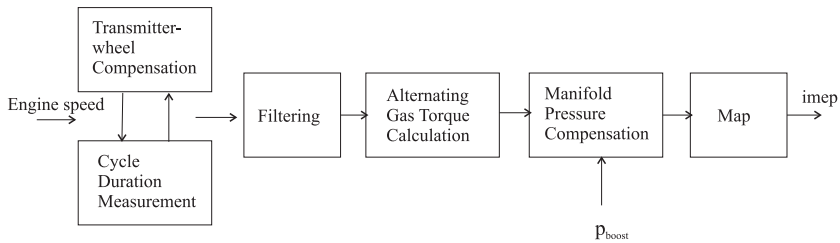

Figure 3.1: Model approach

Input to the model is the engine speed and output is the indicated pressure $imep$. The engine speed signal is recieved with a hall sensor from a transmitterwheel seen in Figure (3.2).
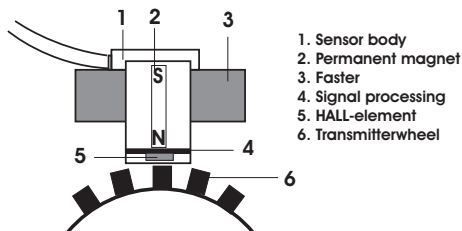

Figure 3.2: Hall sensor

5

After processing the transmitterwheel signal a compensation for production errors on the transmitterwheel must be done (Figure 3.1 'Transmitterwheel Compensation'). The error can be up to 0.5 degrees per tooth and the result is useless without compensation of the errors. From the compensated transmitterwheel signal the angle velocity is estimated via a finite automaton algorithm, see Chapter 7.3, and the angular acceleration is calculated through differentiation of the velocity (Figure 3.1 'Cycle Duration Measurement'). The angle is estimated between the edges from the angular velocity. The transmitterwheel compensation block is executed parallel to the cycle duration measurement until enough data are collected to calculate the correction factors and perform the compensation. The estimated signals are filtered to reduce noise interference (Figure 3.1 'Filtering') and the alternating gas torque is calculated, see Chapter 4 (Figure 3.1 'Gas Torque Calculation'). The data have been filtered off-line with a averaging filter and different filter technics are not investigated in this thesis. If the engine has a turbocharger a manifold pressure compensation is done (Figure 3.1 'Manifold Pressure Compensation') before the indicated pressure can be extracted from maps. Finally the indicated torque can be obtained from the indicated pressure.

Chapter 4

Alternating Gas Torque Calculation

This chapter deals with the alternating gas torque block in Figure (3.1). The alternating gas torque is the gas torque without its the mean value, in analogy with a current without its DC part. Here the equations needed to calculate the indicated engine torque from the engine speed are deduced and explained.

The base for the alternating gas torque is the torque balance at the crankshaft as seen in Equation (4.1) where T_g is the gas torque, T_{mass} is the torque originated from the oscillating and rotating masses, T_l is the load torque and T_f is torque loss due to friction. Assumptions are made for a rigid crankshaft and a sufficiently decoupled power train. This means that all influence on the power train coming from the vehicles mass and gearbox is seen as a torque included in the load torque.

$$T_g - T_{mass} - T_l - T_f = 0 \qquad (4.1)$$

The gas torque, T_g, can be split in one alternating and one direct part, where the direct part is the mean value.

$$T_g = \tilde{T}_g + \bar{T}_g \qquad (4.2)$$

For the method, developed by IAV GmbH, Frauenhofer-Institut and Audi AG which is investigated here, conclusions of the indicated pressure are drawn from the alternating gas torque, see [6]. The stationary case with the direct gas torque, the friction torque and the load torque in balance leads to

$$T_{mass} = \tilde{T}_g \qquad (4.3)$$

It has also been shown through tests that assuming stationarity is a good approximation over a combustion cycle during transient behaviour, see [6], that means that

$$\tilde{T}_g >> \bar{T}_g - \bar{T}_f - \bar{T}_l \tag{4.4}$$

and hence it is possible to draw conclusions of the total engine torque from $\tilde{T}_g$ even in the transient case. The mass torque can be calculated from the kinetic energy of the masses in motion. The kinetic energy can be expressed as:

$$E_{mass} = \int_0^{2\pi} T_{mass} d\varphi = \frac{1}{2}\Theta\dot{\varphi}^2 \tag{4.5}$$

which through differentiation with respect to the crankshaft angle becomes the mass torque with $\ddot{\varphi}$ as the angular acceleration, $\dot{\varphi}$ as the angular velocity, Θ as the mass moment of inertia and Θ' as the derivative of the mass moment of inertia with respect to the crank shaft angle.

$$T_{mass} = \frac{dE_{mass}}{d\varphi} = \Theta\ddot{\varphi} + \frac{1}{2}\Theta'\dot{\varphi}^2 \tag{4.6}$$

From Equation (4.3) and (4.6) an expression for $\tilde{T}_g$, dependent of the engine speed, can be obtained.

$$\Theta\ddot{\varphi} + \frac{1}{2}\Theta'\dot{\varphi}^2 \approx \tilde{T}_g \tag{4.7}$$

$\Theta\ddot{\varphi}$ represents the torque from the rotating masses and $\frac{1}{2}\Theta'\dot{\varphi}^2$ represents the torque from the oscillating masses, see [3]. The piston performs only an oscillating movement, the crankshaft only a rotational movement and the piston rod both an oscillating and a rotating movement. It has been shown through tests that the integration of the alternating gas torque over a combustion cycle is proportional to the energy transformation and hence to $imep$ [6]. Through integration of the mass torque over a combustion cycle with φ_0=720° the help variable effective net torque, T_{eff}, is calculated from Equation (4.8). The effective netto torque is assumed proportional to the energy transformation and hence proportional to $imep$.

$$T_{eff} = \sqrt{\frac{1}{\varphi_0}\int_0^{\varphi_0}(\Theta\ddot{\varphi} + \frac{1}{2}\Theta'\dot{\varphi}^2)d\varphi} \approx \sqrt{\frac{1}{\varphi_0}\int_0^{\varphi_0}\tilde{T}_g d\varphi} \tag{4.8}$$

This relationship is used to create a map where measured values of the mean engine speed, n, and calculated values of the effective net torque are assigned to measured values of the load torque.

$$T_{load} = f(T_{eff}, n) \tag{4.9}$$

The extracted load torque is used together with the calculated mean engine speed as input to a second map where the indicated pressure is extracted.

$$imep = f(T_{load}, n) \tag{4.10}$$

From indicated pressure it is possible to calculate the indicated torque.

The two signals needed to get the indicated pressure are the engine speed, which can be measured, and the effective torque that is calculated from Equation (4.8). To calculate the effective torque the moment of inertia must be known.

4.1 Derivation of the Moment of Inertia

Here follows a review of the calculation of the mass moment of inertia and the derivation of the mass moment of inertia with respect to the crankshaft angle for a one cylinder engine. The one cylinder model is then expanded to fit the six cylinder test bed engine.

To find the moment of inertia all oscillating masses and all rotating masses are summed into one oscillating and one rotating mass. The piston rod mass is represented with one oscillating and one rotating mass as in Figure 4.1, the crankshaft mass is seen as strict rotating and the piston mass as strict oscillating. The kinetic energy in Equation (4.11) is the starting point.
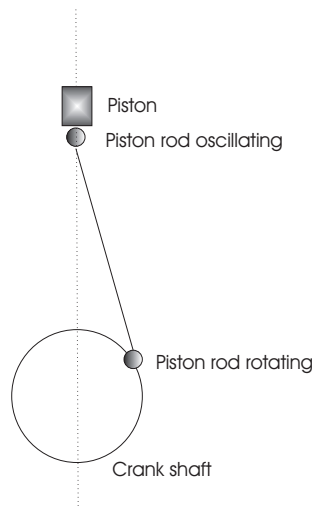
Figure 4.1: Piston rod mass split

$$\int T \cdot d\varphi = \frac{1}{2}m_{rot}v_{rot}^2 + \frac{1}{2}m_{osc}v_{osc}^2 \qquad (4.11)$$

The velocity for the oscillating and rotating masses are expressed through the coordinate systems in Figure 4.2.
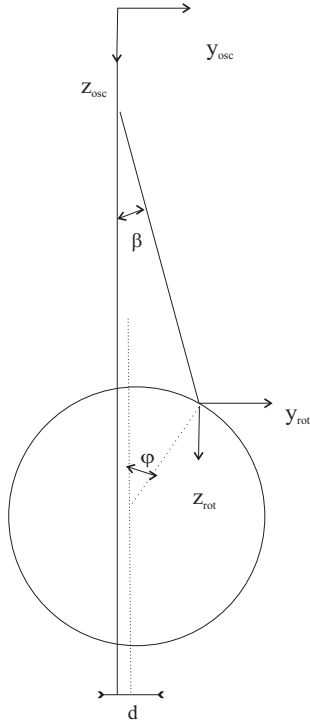
Figure 4.2: Coordinates to describe the mass effect on the piston rod

$$v_{rot}^2 = \dot{z}_{rot}^2 + \dot{y}_{rot}^2 \tag{4.12}$$

$$v_{osc}^2 = \dot{z}_{osc}^2 + \dot{y}_{osc}^2 \tag{4.13}$$

$$z_{rot} = r(1 - \cos\varphi) \tag{4.14}$$

$$\dot{z}_{rot} = r\sin\varphi\dot{\varphi} \tag{4.15}$$

$$\ddot{z}_{rot} = r(\sin\varphi\ddot{\varphi} + \cos\varphi\dot{\varphi}^2) \tag{4.16}$$

$$y_{rot} = r\sin\varphi \tag{4.17}$$

$$\dot{y}_{rot} = r\cos\varphi\dot{\varphi} \tag{4.18}$$

$$\ddot{y}_{rot} = r(\cos\varphi\ddot{\varphi} - \sin\varphi\dot{\varphi}^2) \tag{4.19}$$

x is defined as the piston distance ratio, $x = \frac{s}{r}$ where s is the piston distance measured from the top dead center and r is as in Figure 4.5. $x' = \frac{dx}{d\varphi}$ is the piston velocity ratio, and $x'' = \frac{d^2x}{d\varphi^2}$ piston acceleration ratio.

$$z_{osc} = rx \tag{4.20}$$

$$\dot{z}_{osc} = rx'\dot{\varphi} \tag{4.21}$$

$$\ddot{z}_{osc} = r(x'\ddot{\varphi} + x''\dot{\varphi}^2) \tag{4.22}$$

$$y_{osc} = 0 \tag{4.23}$$

Differentiation of Equation (4.11) with respect to the time leads to Equation (4.24).

$$T\dot{\varphi} = m_{rot}v_{rot}\dot{v}_{rot} + m_{osc}v_{osc}\dot{v}_{osc} \tag{4.24}$$

The velocity for the rotating and oscillating masses can be written as Equation (4.25) and (4.26).

$$v_{osc} = \dot{z}_{osc} \Rightarrow \dot{v}_{osc} = \ddot{z}_{osc} \tag{4.25}$$

$$v_{rot} = \sqrt{\dot{z}_{rot}^2 + \dot{y}_{rot}^2} \Rightarrow \dot{v}_{rot} = \frac{\dot{z}_{rot}\ddot{z}_{rot} + \dot{y}_{rot}\ddot{y}_{rot}}{\sqrt{\dot{z}_{rot}^2 + \dot{y}_{rot}^2}} \tag{4.26}$$

Equation (4.25) and (4.26) in (4.24) leads to the expression below.

$$T\dot{\varphi} = m_{rot}(\dot{z}_{rot}\ddot{z}_{rot} + \dot{y}_{rot}\ddot{y}_{rot}) + m_{osc}\dot{z}_{osc}\ddot{z}_{osc} \tag{4.27}$$

With Equation (4.15), (4.16), (4.18), (4.19), (4.21), (4.22) in Equation (4.27)

$$T = \ddot{\varphi}(r^2m_{rot} + m_{osc}r^2x'^2) + \dot{\varphi}^2(m_{osc}r^2x'x'') \tag{4.28}$$

the moment of inertia for a one cylinder engine is identified from equation (4.7)

$$\Theta = m_{rot}r^2 + m_{osc}r^2x'^2 \tag{4.29}$$

and so is the derivative of the mass moment of inertia with respect to the crankshaft angle

$$\Theta' = \frac{d\Theta}{d\varphi} = 2m_{osc}x'x''r^2 \tag{4.30}$$
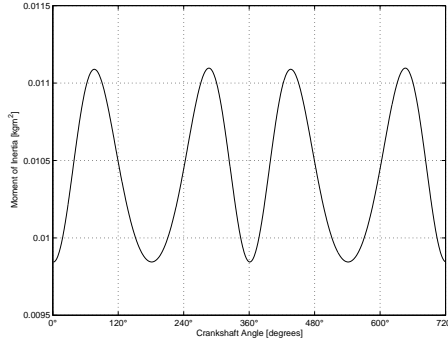
Figure 4.3: The moment of inertia for a one cylinder engine
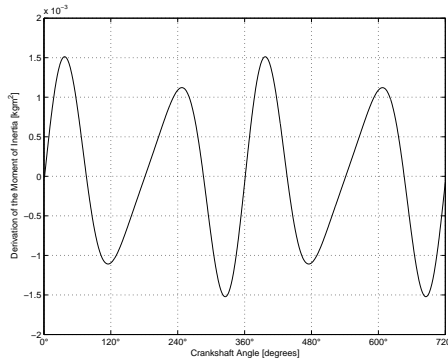
Figure 4.4: The derivative of the moment of inertia w.r.t the crankshaft angle

How the moment of inertia and the derivative of the moment of inertia change
with respect to the crankshaft angle can be seen in Figure 4.3 and 4.4. The
engine data are taken from the test engine.

The piston distance ratio $x = \frac{s}{r}$ can be rewritten through the geometrical
relations found in Figure 4.5, using Equation 4.31 and 4.32. x' and x'' are
calculated through differentiation of x with respect to the crankshaft angle.

Notice that a displacement, d, as in Figure 4.5 is defined as a negative dis-
placement.

$$s = \sqrt{l^2 - d^2} + r - l \cos \beta - r \cos \varphi \qquad (4.31)$$

$$r \sin \varphi = d + l \sin \beta \qquad (4.32)$$

This result in Equation (4.33).
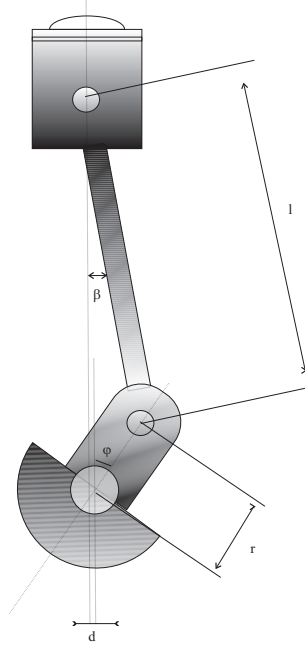
Figure 4.5: System Geometry

$$x = \frac{s}{r} = \frac{\sqrt{l^2 - d^2} + r - l\cos\beta - r\cos\varphi}{r}$$

$$= 1 + \frac{l}{r}\sqrt{1 - \frac{d^2}{r^2}} - \frac{l}{r}\cos\beta - \cos\varphi \tag{4.33}$$

Equation (4.32) squared

$$(r\sin\varphi)^2 = (d + l\sin\beta)^2 \Rightarrow r^2\sin^2\varphi = d^2 + 2dl\sin\varphi + l^2\sin^2\beta \tag{4.34}$$

together with the trigonometric identity

$$\sin^2\beta = 1 - \cos^2\beta \tag{4.35}$$

expresses the angle β as

$$\cos^2\beta = 1 + \frac{2dr}{l^2}\sin\varphi - \frac{d^2}{l^2} - \frac{r^2}{l^2}\sin^2\varphi \tag{4.36}$$

With $\xi = \frac{r}{l}$ and $\mu = \frac{d}{l}$ the piston distance ratio is defined by:

$$x = 1 + \frac{1}{\xi}\sqrt{1 - \mu^2} - \frac{1}{\xi}\sqrt{1 + 2\xi\mu\sin\varphi - \xi^2\sin^2\varphi - \mu^2} - \cos\varphi \quad (4.37)$$

Through one respectively two differentiations with respect to the crankshaft angle the piston velocity ratio (Equation (4.38)) and piston acceleration ratio (Equation (4.39)) are deduced.

$$x' = \left(\frac{dx}{d\varphi}\right) = \sin\varphi + \frac{\xi\sin\varphi\cos\varphi - \mu\cos\varphi}{\sqrt{1 - \xi^2\sin^2\varphi + 2\xi\mu\sin\varphi - \mu^2}} \quad (4.38)$$

$$x'' = \cos\varphi + \frac{\xi\cos^2\varphi - \xi\sin^2\varphi + \xi^3\sin^4\varphi + 3\xi\mu^2\sin^2\varphi}{(\sqrt{1 - \xi^2\sin^2\varphi + 2\xi\mu\sin\varphi - \mu^2})^3}$$
$$- \frac{3\xi^2\mu\sin^3\varphi + \mu\sin\varphi - \mu^3\sin\varphi}{(\sqrt{1 - \xi^2\sin^2\varphi + 2\xi\mu\sin\varphi - \mu^2})^3} \quad (4.39)$$

With the geometry for the test engine used in this thesis the different ratios, x, x', x'', over a combustion cycle are visualised in Figure 4.6. Between 60-90 degrees the velocity ratio has its highest values. In this range the mass forces contributes at most to the angle velocity variations.
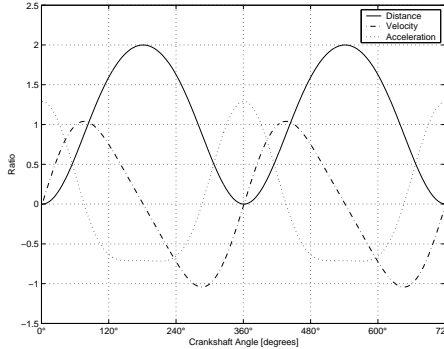
Figure 4.6: Distance (x), velocity (x') and acceleration (x'') ratio

x, x' and x'' are used in Equation (4.29) and (4.30) to calculate the moment of inertia and the derivative of the moment of inertia.

4.1.1 Expansion to a Six Cylinder Engine

The moment of inertia deduced in the last section is for a one cylinder engine. If there are more pistons attached to the crankshaft they are also contributing

to the mass moment of inertia and their contribution change with respect to the crankshaft angle. Because of the 120° shift between the piston cycles and the assumption of a rigid crankshaft the moment of inertia for a six cylinder engine can be calculated from the moment of inertia of a one cylinder engine (Equation 4.29) shifted six times with 120° and then superposed. How the six cylinder moment of inertia and its derivation change with respect to the crankshaft angle can be seen in Figure 4.7 and 4.8.
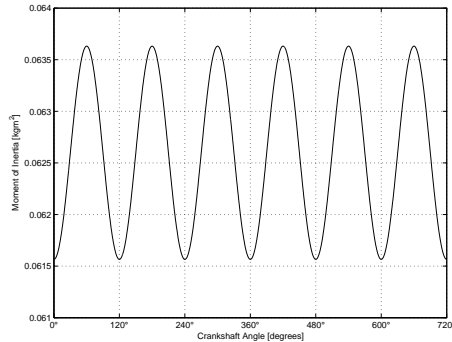

Figure 4.7: The moment of inertia for the six cylinder engine M272
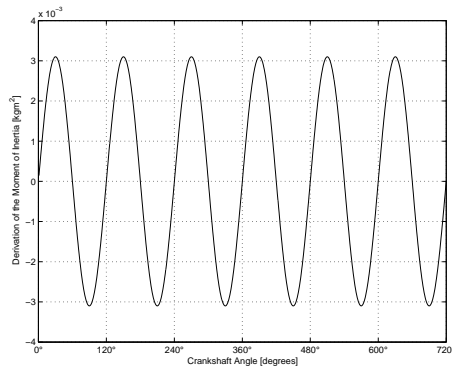
Figure 4.8: The derivative of the moment of inertia for the six cylinder engine M272

4.2 Indicated Pressure to Indicated Torque

To calculate the indicated torque from the indicated pressure one can first calculate the indicated power and therefrom the torque. To get the indicated

power the connection between power, force and velocity seen in Equation
(4.40) is used. The velocity is expressed as $\frac{s}{t}$ where s is the travel distance
for the piston over a combustion cycle and t the cycle time, that is the time it
takes to fulfil a combustion cycle.

$$P = F \cdot \frac{s}{t} \tag{4.40}$$

The force on the piston from the ignition at the time between the first and
second stroke in the combustion cycle (see Chapter 2) can be calculated from
the indicated pressure and the piston area A.

$$F = A \cdot imep \tag{4.41}$$

The cycle time, Equation (4.42), is the time between two consecutive igni-
tions and is calculated from the engine speed n. For one particular piston an
ignition happens once every combustion cycle.

$$t = \frac{1}{\frac{n}{60}} \cdot 2 \tag{4.42}$$

With z as the number of cylinders Equation (4.40) can be written as Equation
(4.43).

$$P_i = \frac{A \cdot imep \cdot s \cdot n \cdot z}{2 \cdot 60} \tag{4.43}$$

Since the indicated pressure is in $[bar]$ a correction must be made to get the
final expression in $[W]$. After reduction and a correction for $[m] = 10[dm]$
the pressure is in $[W]$ and calculated from Equation (4.44) with V_d as the
displacement volume.

$$P_i = \frac{V_d \cdot imep \cdot n}{1.2} \tag{4.44}$$

Now the indicated torque can be calculated through Equation (4.45).

$$T_i = \frac{P_i}{\omega} = \frac{100 V_d \cdot imep}{4\pi} \tag{4.45}$$

Chapter 5

Manifold Pressure Dependence

This chapter concerns the manifold pressure dependence block in Figure 3.1. The model should provide accurate information independently of it is an engine with turbocharger or not. A turbocharger provides a higher alternating gas torque amplitude which could cause problems concerning the map extraction. This is not considered in this thesis because the engine used for the measurements does not have a turbocharger. If an engine with turbocharger should be investigated, the manifold pressure dependence could be normalizied by a map that normalizes the alternating gas torque amplitude and make it independent from manifold pressure as described in [6]. It is a linear relationship (Figure 5) which also make the gas torque independent of the atmosphere pressure.
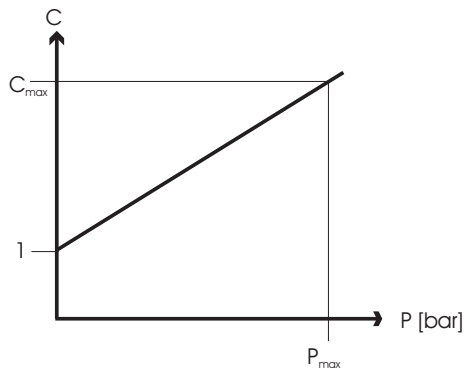

Figure 5.1: Linear manifold pressure dependence

The compensation factor is extracted from a map and multiplied with alternating gas torque, as in Equation (5.1), resulting in a compensated gas torque. The compensated gas torque is used as input for the indicated torque map.

$$\tilde{M}_{g_{compensated}} = \frac{\tilde{M}_g}{c} \tag{5.1}$$

Chapter 6

Transmitterwheel Error Compensation

In this chapter a method to compensate for the transmitterwheel error is presented. The compensation is represented by the transmitter wheel error block in Figure 3.1. One source that affects the accuracy of the angular velocity calculation are the teeth partition defects of the transmitterwheel that can arise in production, see Figure 6.1. This error is different for every tooth on the transmitterwheel. The error can be up to $0.5°$ [7] and must be taken into account and compensated for.
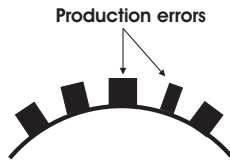
Figure 6.1: Different width between the teeth

To be able to do this the behaviour of the the engine speed over a combustion cycle must be known. For this purpose a model built in Matlab/Simulink is used when solving Equation 6.1 (the same equation as 4.7, but now with load and friction torque as one variable, $T_{lf} = T_l + T_f$) numerically. From the obtained angle acceleration the angle velocity is then calculated through integration.

$$\ddot{\varphi} = \frac{1}{2} \frac{\Theta'(\varphi)}{\Theta(\varphi)} \cdot \dot{\varphi}^2 - \frac{T_g(\varphi)}{\Theta(\varphi)} - \frac{T_{lf}}{\Theta(\varphi)} \qquad (6.1)$$

More about the model is to be read in [4]. The mass torque is modeled from Equation (4.6) and the load and friction torque are set to zero as approxi-

mation of the forces from the street almost equals the friction forces over a combustion cycle during motored cycles. Therefore only data obtained during motored cycles can be used to calculate the correction factors, which are the aim of this transmitterwheel compensation algorithm. The gas torque is calculated from Equation 6.2 [1].

$$T_g = (p_{cyl} - p_0)A_p\frac{ds}{d\varphi} \tag{6.2}$$

A_p is the piston area, p_{cyl} is the pressure in the cylinder and p_0 is the atmosphere pressure. The cylinder pressure is crankshaft angle dependent and calculated for one cylinder and then shifted six times $120°$ and superposed to fit a six cylinder engine [1]. With T_g and T_{mass} known the simulink model is used to solve Equation (6.1) which gives an approximation of the engine speed. Below are three figures that show the engine speed during motored cycles. Here interesting changes in the behavior of the engine speed at low, middle and high engine speed can be seen. Since no effort has been put in the parametrisation of the engine speed model the values on the y-axis are incorrect and only the relation between the engine speeds in the three figures are of interest.
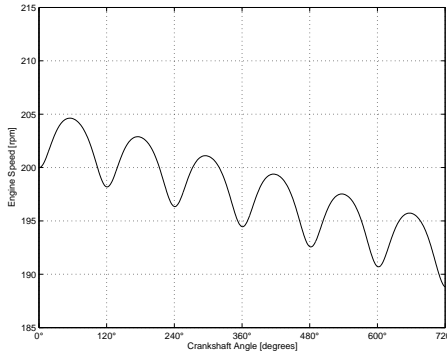

Figure 6.2: Behavior of low engine speed during motored cycles
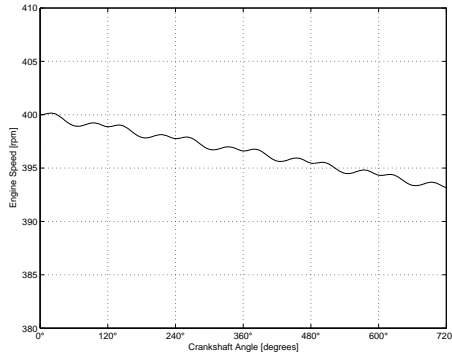
Figure 6.3: Behavior of the engine speed when the gas and mass forces are in balance
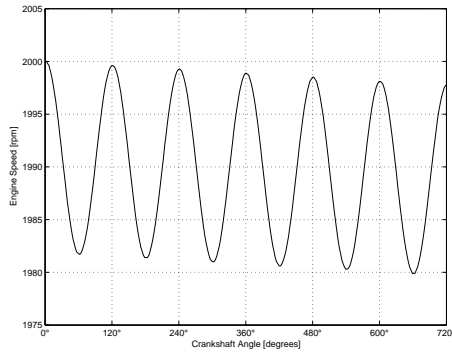
Figure 6.4: Behavior of high engine speed during motored cycles

The mass torque and the gas torque works against each other. The oscillations at low engine speeds, Figure 6.2, are caused by the gas torque. With increasing engine speed the mass torque contribution increase and because of the opposite direction from the gas torque they are in balance at a certain engine speed which means there are almost no oscillations, Figure 6.3. At high engine speeds the mass torque is much higher than the gas torque and causes sine formed oscillations, Figure 6.4. These properties of the engine speed can be used in different ways to compensate for the transmitter wheel error.

6.1 Using the Sine behaviour of the Engine Speed

As seen in Figure 6.4 the engine speed behaves like a sine curve at higher mean engine speeds at motored cycles. This knowledge can be used to de-

termine the transmitterwheel error for every single tooth. This is done by
measuring the angular velocity for every tooth on the transmitterwheel over
a whole combustion cycle during motored cycles, see Equation (6.3), at a
mean engine speed high enough to produce a sine wave. The load and fric-
tion torque and the quantisation errors are not periodic and their effect on a
special tooth is seen as stochastic disturbance which can be reduced through
averaging.

$$\bar{\omega} = \begin{pmatrix} \omega_1 \\ \omega_2 \\ \vdots \\ \omega_{120} \end{pmatrix} \tag{6.3}$$

The time for every tooth is calculated from the angular velocity in Equation
(6.4).

$$\bar{t} = \bar{\omega}^{-1} = \begin{pmatrix} t_1 \\ t_2 \\ \vdots \\ t_{120} \end{pmatrix}^t \tag{6.4}$$

To get a measure of how constant the mean engine speed is over the combus-
tion cycle, the variance for the time vector is calculated in Equation (6.5). The
more constant the engine speed is the less engine speed change correction, see
Figure 6.6, must be done.

$$var(\bar{t}) = \frac{1}{k} \sum_{i=1}^{k} (t(i) - \langle t \rangle)^2 \qquad k = 120 \tag{6.5}$$

The procedure is then repeated from the beginning and the variance from the
latest time vector is always compared with the lowest variance from the ear-
lier vectors. If the variance is lower, the new time vector is saved and the
other is erased. After x combustion cycles, with x chosen properly, the mean
engine speed is considered constant enough, and its corresponding time vec-
tor, $\mathbf{t}_{teeth}$, is saved. To make the method more insensitive towards stochastic
disturbances like misfire in one of the cylinders, changes in the load torque
and quantisation errors a number of $\mathbf{t}_{teeth}$ are calculated and an average is
generated as in Equation (6.6).

$$\bar{t}_{average} = \frac{\bar{t}_{teeth_1} + \bar{t}_{teeth_2} + \ldots + \bar{t}_{teeth_m}}{m} \tag{6.6}$$

Based on a perfect transmitterwheel, and with the assumption that the engine
speed is a sine wave during motored cycles, the frequency component of the
measured engine speed that corresponds to the perfect engine speed is de-
rived via fourier series representation. Equation (6.7) represents the intended

oscillation in the engine speed. The fourier series works like a filter, which represents the shape of a perfect engine speed signal (Figure 6.5), that filters out everything corresponding to the perfect alternating engine speed from the measured engine speed, ω, leaving only the direct engine speed and the error, see Equation (6.9). A six cylinder engine is assumed here, but the method is adaptable to any engine size.

$$\bar{F}_k = \sin\left(\frac{3 \cdot 2\pi}{360} \cdot \bar{k}\right), \qquad k = 0, 6, \ldots, 714 \tag{6.7}$$
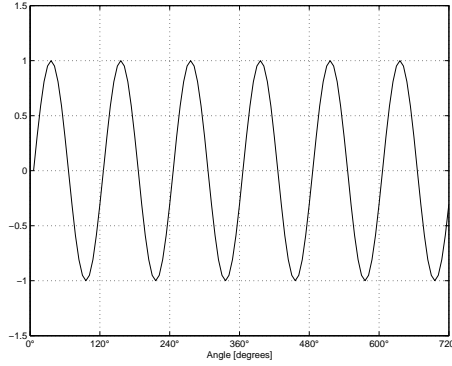

Figure 6.5: Fourier filter

The fourier coefficient a_0 is the amplitude of the sine curve part of the alternating engine speed and is calculated in Equation (6.8).

$$a_0 = \frac{1}{60} \sum_{i=1}^{N-1} F_k(i) \cdot \omega_{total}(i), \qquad \bar{\omega}_{total} = (\bar{t}_{average}^{-1})^t \tag{6.8}$$

The alternating engine speed is subtracted from the total engine speed as in Equation (6.9) leaving only the direct part and noise caused by the errors.

$$\bar{\omega}_{direct} = \bar{\omega}_{total} - a_0\bar{F} = <\omega_{total}> + \bar{\zeta} \tag{6.9}$$

$\bar{\zeta}$ is the noise caused by the tooth errors.

$$\bar{t}_{direct} = (\bar{\omega}_{direct}^{-1})^t \tag{6.10}$$

Since it is not likely to find a time vector with a constant average value over the whole combustion cycle, compensation for changes in the mean engine speed during the combustion cycle must be done. The time error vector is therefore split in two parts, one for the first revolution, R1, and one for the second, R2.

$$\bar{t}_{direct_1} = \begin{pmatrix} t_{direct_1} \\ t_{direct_2} \\ \vdots \\ t_{direct_{60}} \end{pmatrix} \qquad \bar{t}_{direct_2} = \begin{pmatrix} t_{direct_{61}} \\ t_{direct_{62}} \\ \vdots \\ t_{direct_{120}} \end{pmatrix}$$

The mean engine speed difference between R2 and R1 is calculated by Equation (6.11).

$$\omega_{change} = \frac{60}{\sum \mathbf{t}_{direct_2}} - \frac{60}{\sum \mathbf{t}_{direct_1}} \tag{6.11}$$
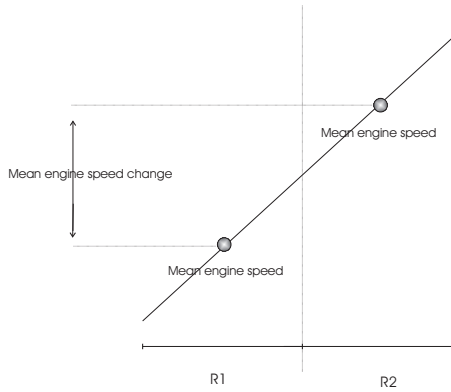

Figure 6.6: Engine speed change, first and second revolution

The mean engine speed change is assumed linear over the combustion cycle as seen in Figure 6.6. Correction for the change is made for R2 and the engine speed with errors is distributed evenly over all teeth in equation (6.12), see Figure 6.7. This gives the engine speed for every tooth on the transmitterwheel like it would be if there was no transmitterwheel errors.

$$\bar{\omega}_{correct} = \omega_{change} \cdot \frac{1}{60} \cdot \begin{pmatrix} 1 \\ 2 \\ \vdots \\ 60 \end{pmatrix} + \left(\frac{60}{\sum \bar{t}_{direct_2}} - \frac{1}{2}\omega_{change} \right) \tag{6.12}$$

For easy correction of the measured time between two flanks, a correction factor is calculated.

$$\bar{K} = \begin{pmatrix} K_1 \\ K_2 \\ \vdots \\ K_{60} \end{pmatrix} = 1 - (\bar{t}_{direct_2} - \bar{\omega}_{correct}^{-1})\bar{\omega}_{correct} \tag{6.13}$$
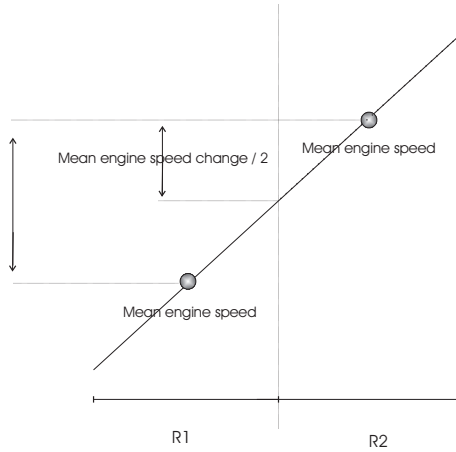
Figure 6.7: Engine speed change, linear distributed

The correction factor is multiplied with its corresponding time to get correct time and engine speed measurements. If it is only 58 teeth on the ransmitter-wheel there will be only 58 correction factors.

6.2 Using the Opposite Phase of the Gas and Mass Torque

Another approach for correction of transmitterwheel errors has been developed by Frauenhofer-Institut für Informations- und Datenverarbeitung (ITTB) and is described in [7]. The approach uses the opposite phase of the gas and mass torque, see Figure 6.3, to find out the geometry defects on the transmitterwheel and compensate for them. First a specific engine speed range is defined, from n_{min} to n_{max}, in which the gas and mass torque oscillations are balanced in average. Then the length between two teeth are estimated by multiply the measured time, $t_n = \frac{1}{f_n}$, with the estimated angular velocity, ω_n. The angular velocity is estimated as the mean engine speed.

$$\varphi_{n_{error}}(z) = t_n(z) \cdot \omega_n = \frac{\omega_n}{f_n(z)} \tag{6.14}$$

Here $\varphi_{n_{error}}$ is the length of gap z with the error, z is the tooth gap index and $f_n(z)$ is the measure frequency for this gap.

To get the relative error, $\delta_{error}(z)$, for a gap z the estimated incremental length is subtracted with the ideal incremental length, φ_z, and a mean average over the upper and lower engine speed bound is calculated to even the effects from the gas and mass torque.

$$\bar{\delta}_{error} = \frac{1}{n_{max} - n_{min}} \sum_{n=n_{min}}^{n_{max}} \left[\frac{\omega_n}{\bar{f}_n} - \varphi_z \right] \tag{6.15}$$

$$\bar{K} = 1 + \bar{\delta}_{error} \frac{30}{\pi} \tag{6.16}$$

In this approach it is assumed that the gas and mass torque are in perfect balance over a specific engine speed range. One advantage with this approach is the low complexity and that it is parameter independent.

Chapter 7

Cycle Duration Measurements

The cycle duration measurement block in Figure 3.1 is the part of the model where the angle, angular velocity and angular acceleration are measured and estimated from the hall signal and which are then used in the block 'alternating gas torque' for calculations (see Chapter 4).

7.1 Adjustments for the Edge Signal Gap

The output from the hall sensor is a signal with an edge for every occuring tooth. To handle the abnormality of the two teeth gap in this edge signal, see Figure 7.1, the torque calculations must be delayed at least 18 degrees so the first tooth on the new revolution occurs after the gap before new calculations can be done.
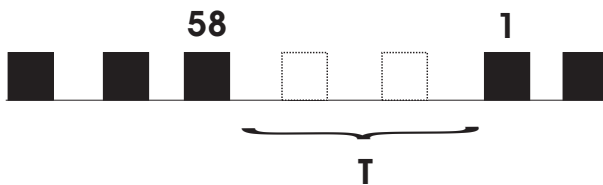

Figure 7.1: Signal with 58 teeth

7.2   Estimation of the Crankshaft Angle and Speed

To get a sufficiently good estimation of the angle, angle velocity and angle acceleration in, three different approaches are considered. Two of them are based on assumptions about the velocity and acceleration between two positive edges. In the first approach constant acceleration is assumed so that the angle and angular velocity are recalculated at every sample time. The second approach assumes constant angular velocity and only the angle is recalculated at every sample time. The third approach makes use of the first two approaches, but makes an update of angle, angle speed and angle acceleration only every six degrees.

7.2.1   Estimation with Constant Angular Acceleration

For the first approach the angle acceleration, α, is estimated from the angular velocity at edge i and $i-1$, as in Equation (7.1) where $\Delta t = t_i - t_{i-1}$.

$$\alpha_i = \frac{\omega_i - \omega_{i-1}}{\Delta t} \tag{7.1}$$

The angular acceleration is then assumed constant to the next edge $i+1$, see Figure 7.2. Now the angular velocity between edge i and $i+1$ can be estimated at every sample n where n is the reference signal in Figure 7.5.

$$\omega(n) = \omega(n-1) + \alpha_i \cdot t_{samp} \tag{7.2}$$

The angle is calculated with the estimated velocity.

$$\varphi(n) = \varphi(n-1) + (\omega(n) - \omega(n-1)) \cdot t_{samp} \tag{7.3}$$
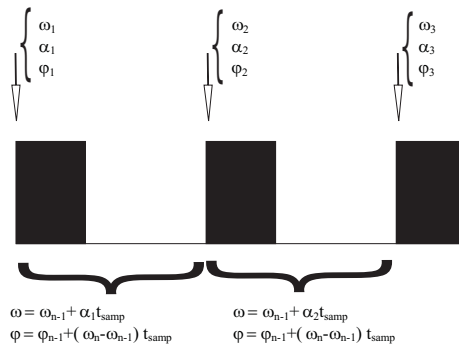

Figure 7.2: Constant angular acceleration between the edges

7.2.2 Estimation with Constant Angular Velocity

For the second approach the calculated velocity at edge i is considered constant until edge $i + 1$. Then the angle can be estimated from Equation (7.4) using a counter which counts the number of samples between edge i and $i+1$ (Figure 7.3).

$$\varphi(n) = \varphi(i) + \omega(i) \cdot counter \cdot t_{samp} \qquad (7.4)$$
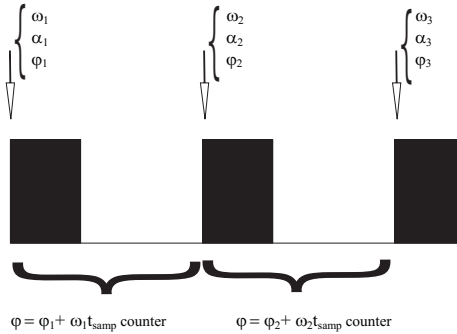
Figure 7.3: Constant angular velocity between the edges

7.2.3 Estimation Every Six Degrees

Tests are also done with a third method with updates and calculations only every positive edge, i.e every six degrees whereas the methods described in 7.2.1 and 7.2.2 interpolates between the edges. This means that no calculations are made between the edges, less calculation means higher model speed but the angle resolution is not better than six degrees, see Figure 7.4. This method is especially interesting since it enables the evaluation of the trade off between loss of accuracy and gain in model calculation time.
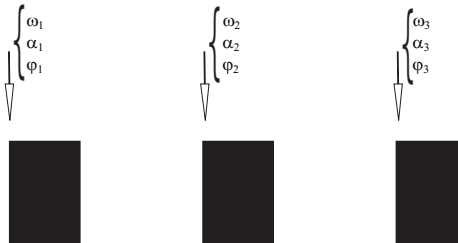
Figure 7.4: Updates only at a positive edge

## 7.3 The Estimation Algoritm Based on Finite Automaton Theory

The estimation algorithm used to calculate the angular velocity at every new edge from the transmitterwheel signal is based on finite automaton theory. It is explained in this section.

The crankshaft angle can be measured only every six degrees, i.e when a positiv edge on the transmitterwheel occurs. The estimation algorithm uses the last calculated angular velocity to decide the position of the crank shaft. The angular velocity is calculated, when a positive edge appears, using this differential equation:

$$\omega = \frac{\Delta\varphi}{\Delta t} \tag{7.5}$$

There are two different approaches of the finite automaton, time synchron and angle synchron. Only the angle synchron engine speed survey is discussed here because of better results in [5].

7.3.1 Angle Synchron Engine Speed Survey

The time interval over an increment angle, e.g $\Delta\varphi = 6°$, is measured with the help of an internal clock that counts the number of samples between two consecutive positive edges.

$$\Delta t = counter \cdot t_{ref} \cdot K, \qquad t_{ref} = t_{samp} \tag{7.6}$$

K is the transmitterwheel error correction factor that is derived in Chapter 6.
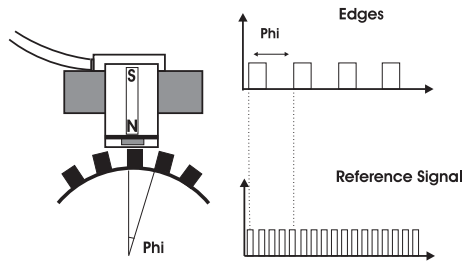

Figure 7.5: Time measurement between two edges

In Figure 7.5 one can see that the accuracy increases with shorter sample time. This also means that the algorithm has a lower accuracy at a higher engine speed because of the decreased time between two flanks.

7.3.2 Forgetting factor

To make the angular velocity and the angular acceleration estimation less noise sensitive a forgetting factor k is used to include information from the former measurements into the new one.

$$\omega_{i_k} = k\omega_i + (1 - k)\omega_{i-1} \tag{7.7}$$

The bigger k is the more trust is put in the new measurement. If the signal is interfered by noise this could result in large deviations between the new calculated angular velocity and its real value. With a smaller k value, less trust is put in the new measurement, would mitigate the impact of the error but make the system dynamic slower. The determination of k is a compromise between system response time and noise sensitivity and it was chosen to k=0.7 through trial and error.

Chapter 8

Measurements in an Engine Test Bed and in Vehicle

To get data for the map construction discussed in Chapter 4, and to model validation, measurements was made in an engine test bed. The data is split up in two parts. One for map constuction and the other one for model validation. The engine speed was measured with an optical sensor every crank angle degree. The indicated pressure, $imep$, was measured with a sensor at different combinations of load torque and engine speed.

The conditions at the test bed were not good enough to give accurate measurements over the whole engine speed spectrum. At the test bed the maximum sample rate, the reference signal in Figure 7.5, was 4MHz. Thus quantisation errors influenced the measurements for higher engine speeds, as seen in Figure 8.1. A sample rate of 4MHz means a new edge in the reference signal every $t_{ref} = \frac{1}{4MHz} = 2.5 \cdot 10^{-7}s$. If the engine speed is $n = 4000rpm = 24000 \ degrees/s$ it takes $t_{crank} = 1/24000 = 4.17 \cdot 10^{-5}s$. for the crankshaft to rotate one degree. Under these conditions the quantisation steps are in the range of $\frac{t_{ref}}{t_{crank}} \cdot n = 0.006 \cdot 4000 = 24rpm$ which correspond to the quantisation steps in Figure 8.1. For lower engine speeds this effect was not as pronounced (Figure 8.2), enabling a satisfactory measuring of the dynamic engine speed. These results, for the lower engine speeds, were used for model validation. As the transmitterwheel compensation needs the transmitterwheel signal with a six degrees resolution for validation, transmitterwheel measurements were made in a test vehicle in addition to the engine test bed measurements.
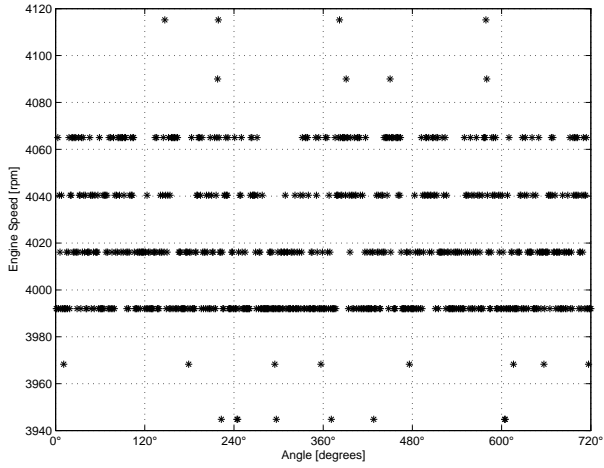
Figure 8.1: The sample points from measurements at high engine speed, 4000 rpm at 100Nm load torque
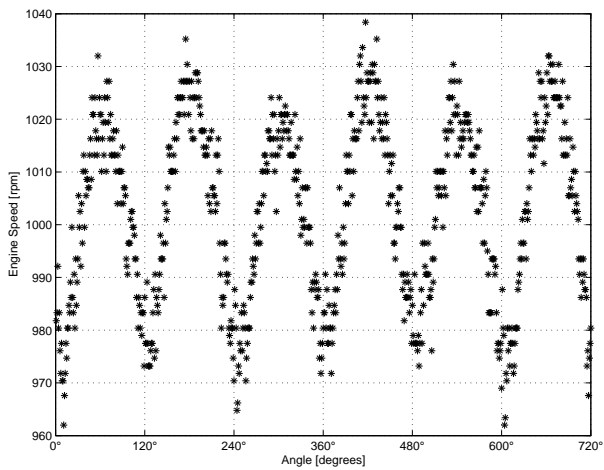
Figure 8.2: The sample points from measurements at low engine speed, 1000 rpm at 100 Nm load torque

8.1   Map construction

Since the quality of the measurements at higher engine speeds were inaccurate the map is limited to engine speeds between 750 rpm to 2000 rpm and the results for an engine speed over 1000 rpm must be evaluated with caution. The relationship between the effective and the load torque seen in Figure 8.3 and the relationship between load torque and indicated pressure at constant engine speed seen in Figure 8.6 are used to create the two needed maps.
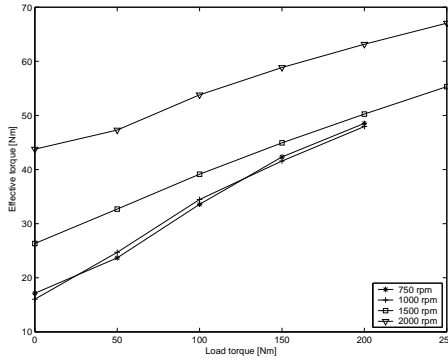
Figure 8.3: The relationship between effective and load torque at constant engine speed
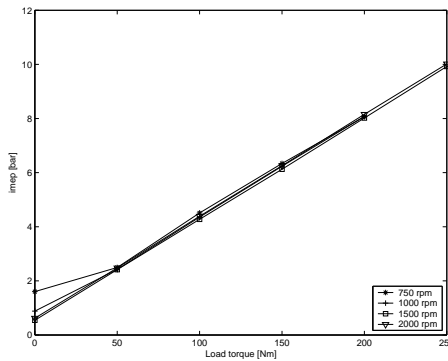
Figure 8.4: The relationship between $imep$ and load torque

In the first map, see Figure 8.6 the calculated effective torque and the mean engine speed are used as input to extract the load torque. After the load torque is extracted from the map it is used as input together with the engine speed to extract the indicated pressure from the final map. The indicated torque is

then calculated from Equation (4.45).
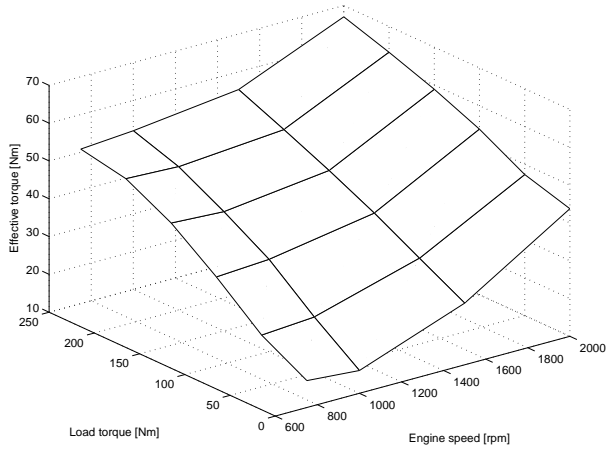
Figure 8.5: Map to extract the load torque
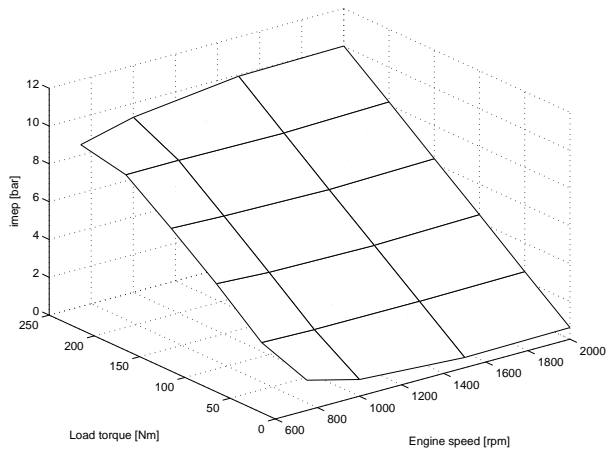
Figure 8.6: Map to extract the $imep$

Chapter 9

Validation and Results

The validation and results of the different estimation approaches, transmitter-wheel error compensation and the complete model are presented.

9.1 Comparison of the Different Angle Estimation Approaches

For the validation of the different approaches for estimating the angular velocity, presented in Chapter 7 an engine model is used. The model has the same parameters as the engine test bed and delivers a processed hall sensor signal with an edge for every tooth.

The first attempt to estimate the angle and angular velocity, as described in Section 7.2.1 did not give the desired results when validated. As seen in Figure 9.1 the angular velocity becomes noisy and through the velocity updates in between the edges errors arise at every transmitterwheel gap. The influence of the gap is seen in the second and the fifth peak in the figure. Another disadvantage is that the interpolation calculations in between the edges makes the approach more complex which would make it hard to realize it on-line. The estimation approach to update the calculations only at every edge, as described in section 7.2.3, gives accurate results for the 58 edges signal with interpolation in the gap, as can be seen in figure 9.2. To update only at every edge demands much less calculations compared with the approaches using interpolation in between the edges and is therefore the approach to use if there are on-line demands.

The original edge signal is used with estimation
as desribed in Section 7.2.1
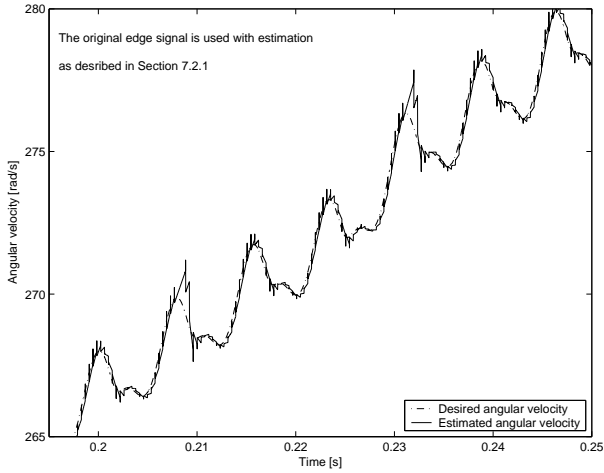
Figure 9.1: The estimated signal is noisy and in the second and fifth peak the influence of the two teeth gap is seen

The original edge signal is used with estimation
as in Section 7.2.2
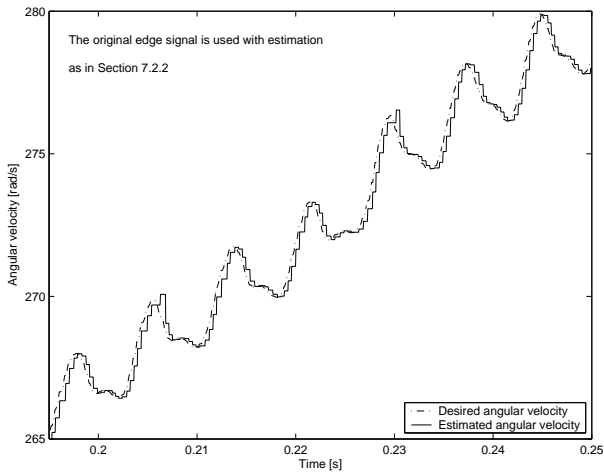
Figure 9.2: The estimated signal fits the desired signal well. In the second and fifth peak the influence of the two teeth gap is smaller then in Figure 9.1

The estimation of the angle with constant angular velocity between the edges, discussed in Section 7.2.2, estimates the angular velocity only at every edge. This approach includes however interpolation of the angle in between the edges and is therefore not suited for on-line use.

The conclusions drawn from the validation with the engine model are that the estimation of the angle with constant angular velocity between the edges and the estimation with updates only at every edge with interpolation in the gap are of further interest. The other methods can be discarded.

9.2   Transmitterwheel Error Compensation Methods

To make the validation of the transmitterwheel error compensation possible a special developed hardware which enables $20MHz$ resolution was used. The engine speed was measured over an inductive sensor in a test vehicle as mentioned in Chapter 8. The measurements were used to validate the transmitterwheel error compensation but not to validate the whole model because the indicated pressure and the load torque could not be measured in the test car.

9.2.1   The Sine Behavior of the Engine Speed

The method validated is presented in Section 6.1. To calculate the correction factors a measurement during motored cycles with the engine speed dropping from 5000 to 1400 rpm was used. As seen in Figure 9.3 the result is not satisfactory. The six combustion variations that ought to be seen over a combustion cycle after compensation are not visible. The reason why the method does not work properly is that the assumption, that the oscillation in the engine speed is a sine curve at high mean engine speed during motored cycles, is false. It means that there are oscillations left in the engine speed when the correction factors are calculated which leads to errors in the correction factors.

9.2.2   The Opposite Phase Of The Gas And Mass Torque

The method using the opposite phase of the gas and mass torque is described in Section 6.1. The correction factors was calculated from engine speed increased from 1400 to 3500 rpm. The boundary for the engine speed in which the gas and mass torque were in balance were found through trial and error and thus chosen to $n_{min} = 1700$ and $n_{max} = 2300$. The result seen in Figure 9.4 is satisfactory and it is possible to detect all six combustion in the engine speed signal. The peaks seen in the signal without compensation says nothing about the combustions and originates from the errors.
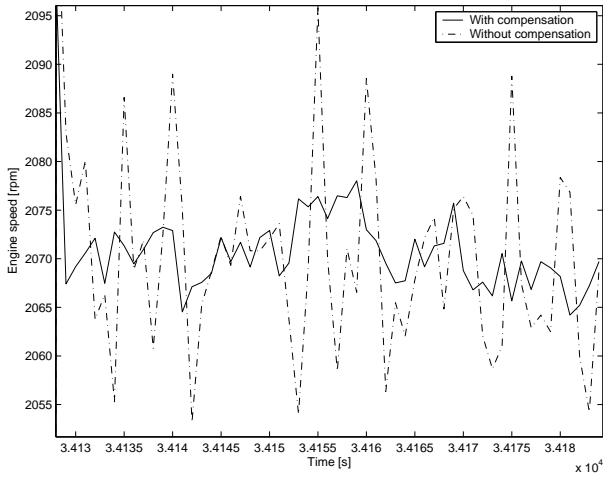
Figure 9.3: Engine speed over a combustion cycle before and after transmitterwheel error compensation.
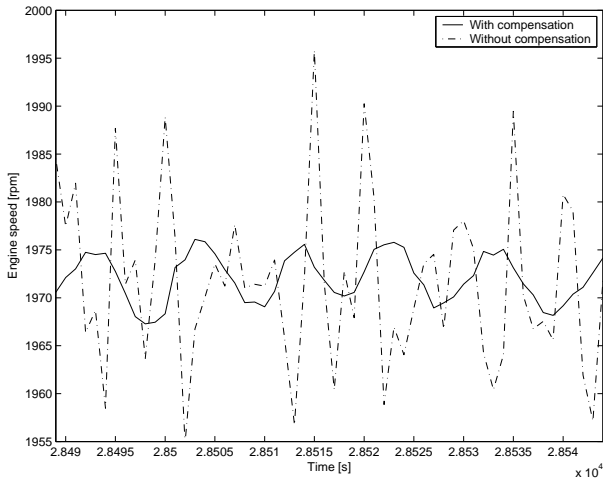
Figure 9.4: Engine speed over a combustion cycle before and after transmitterwheel error compensation.

9.2.3   Summary of Transmitterwheel Compensation Methods

The method validated in Section 9.2.2 gives satisfying results and is thus used to generate a satisfying input signal to the complete torque estimation model which will be validated in Section 9.3. To validate the transmitterwheel error compensation the signal from the transmitterwheel is needed as input. This signal was as mentioned in Section 9.2 measured with an inductive sensor in a test vehicle and is measured in the same way in serie produced cars.

9.3   Validation of the Torque Estimation Model

To validate the model with a six degree signal every six sample from the one degree resolution signal measured in the engine test bed, see Chapter 8, were used. The data used for validation is taken from the remaning part not used when creating the maps.

9.3.1   Updates only Every Six Degrees

Validations at different compositions of load torque and engine speeds were done and an indicated torque mean error, the difference between the estimated and the measured indicated torque, was calculated. In Figure 9.5 the torque error percentage is seen. The error increases from 0.9 % at maximum load to 3.5 % at minimum load at 750 rpm. At 1000 rpm the error is beneath 5 % for loads over 50 Nm. The quantisation errors effects the engine speed measurements more at low loads because of that the amplitude of the oscillations in the engine speed is lower and therefore harder to detect. No conclusions can be drawn from the results at engine speeds higher than 1000 rpm because of the quantisation errors described in Chapter 8.

9.3.2   Constant Angular Velocity between the Edges

Validations were done exactly as by the update every six degree method. The torque error percentage is seen in Figure 9.6. This method delivers a poorly result compared to the one discussed before and is not to go any further with. The result can be explained by that the angle is interpolated between the edges but the angular velocity is not. These gives new values of the angle dependent moment of inertia at every interpolated value of the angle but they are not corresponding to the constant angular velocity which is assumed and therefore errors occurs.
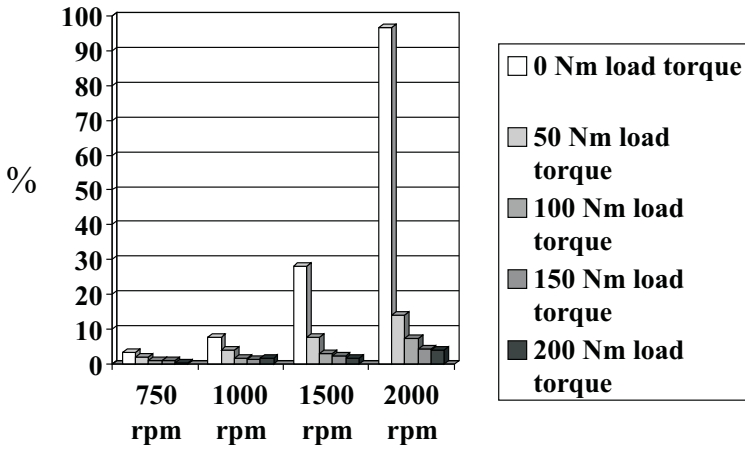
Figure 9.5: The indicated torque error percentage
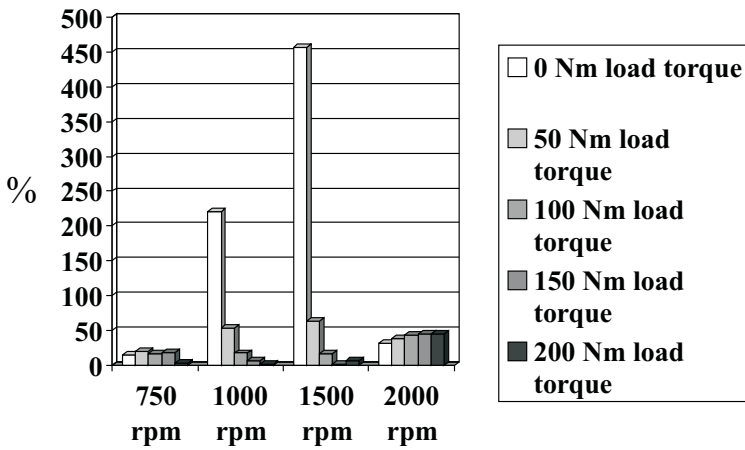
Figure 9.6: The indicated torque error percentage

Chapter 10

Conclusions

The aim of this master thesis was to implement and evaluate a method to estimate the indicated engine torque developed by IAV GmbH, Fraunhofer-Institut and Audi AG. Measurements on an engine test bed was made to construct the needed maps and to get data for validation of the torque estimation model. Measurements in a test vehicle was made to get data for validation of the transmitterwheel error compensation method. The method is based upon engine speed measurements with a resolution high enough to catch the dynamic behavior of the engine speed. With the measurements from the test vehicle the transmitterwheel error compensation method using the opposite phase of the gas and mass torque described in Section 6.2 was succesfully validated, as seen in Section 9.2.2. Using the measurements from the engine test bed, the complete torque estimation method was validated for engine speeds to $1000\ rpm$ with the errors below 5 % except for $1000\ rpm$ with minimal load torque were the error is close to 10 %, see Chapter 9. This is a satisfactory result which could improve the comfort by making manual gearboxes shift smoother. As seen in Figure 9.5 the error at 750 rpm for this row of measurements is between 0.9-3.4 %. The error increases with decreasing load torque because of a greater impact of the remaining transmitterwheel error together with increasing quantisation errors. The amplitude of the oscillations in the engine speed is lower at low load torque and therefore more difficult to catch which can be clearly seen in the model results for lower torques. The update every six degrees method, discussed in Section 7.2.3, which calculates new values of the crank angle, angle velocity and angle acceleration at every new edge of the transmitterwheel signal, gives the best result of the discussed methods, see Chapter 7.

Chapter 11

Future Work

The torque estimation algorithm investigated in this thesis give promising results in the validated engine speed range. To be able to validate the model over the entire engine speed spectra new measurements with higher sample rate must be made. As shown in Section 9.2.2 the transmitterwheel compensation compensates for a large part of the errors but a part will always remain. To minimize these remaining errors an optimization of the engine speed range, in which the gas and mass forces are in balance, is needed. An optimization of the number of combinations of load torque and engine speeds needed to create the maps is also of intrest, as is the improvement of the interpolation algorithm between these combinations of torque and engine speed, to minimize the error in the map output. The validation data was filtered off-line with an averaging filter. To enable filtering on-line an adaptive filter would be required.

References

[1] Hermann Fehrenbach. *Berechnung des Brennraumdruckverlaufes aus der Kurbelwellen-Winkelgeschwindigkeit von Verbrenungsmotoren.* Düsseldorf, Germany, 1991.

[2] John. B. Heywood. *Internal Combustion Engine Fundamentals.* McGraw-Hill, New York, USA, 1998.

[3] U. Kincke and L. Nielsen. *Automotive Control Systems For Engine, Driveline and Vehicle.* Addison-Wesley, Berlin, Germany, 2000.

[4] P. Klein. Entwicklung eines adaptiven regleralgorithmus für eine unwuchtkompensation. Master's thesis, Universität Siegen, Siegen, Germany, 2004.

[5] C. Koch. Entwicklung und vergleich von verfahren zur positionserfassung der kurbelwelle. Master's thesis, Institut für energieeffiziente Systeme, Fachhochschule Tier, Trier, Germany, August 2003.

[6] H. Fehrenbach C. Hohmann T. Schmidt W. Schultalbers H. Rasche. Bestimmung des motordrehmoments aus dem drehzahlsignal. *Motorentechnische Zeitschrift*, (12):1021–1027, December 2002.

[7] H. Fehrenbach C. Hohmann T. Schmidt W. Schultalbers H. Rasche. Verfahren zur kompensation des geberradfehlers im fahrbetrieb. *Motorentechnische Zeitschrift*, (7-8):588–591, July/August 2002.

Notation

Symbols used in the report.

Variables and parameters

$\ddot{\varphi}$	Angular acceleration
$\dot{\varphi}$	Angular velocity
Θ	Mass moment of inertia
Θ'	Derivation of the mass moment of inertia w.r.t the crank shaft angle
$\tilde{T}_g$	Alternating gas torque
$\bar{T}_g$	Direct gas torque
$\bar{T}_f$	Friction torque
$\bar{T}_l$	Load torque
l	Piston rod
ξ	Piston rod ratio
d	Displacement
μ	Displacement ratio
s	Piston distance
$\dot{s}$	Piston velocity
$\ddot{s}$	Piston acceleration
x	Piston distance ratio
x'	Piston velocity ratio
x''	Piston acceleration ratio
A	Piston area
s	Piston distance
t	Cycle time
z	Number of cylinders

Abbreviations

rpm	Revolutions Per Minute
$imep$	Net Mean Effective Indicated Pressure

Copyright

Svenska

Detta dokument hålls tillgängligt på Internet - eller dess framtida ersättare - under en längre tid från publiceringsdatum under förutsättning att inga extraordinära omständigheter uppstår.

Tillgång till dokumentet innebär tillstånd för var och en att läsa, ladda ner, skriva ut enstaka kopior för enskilt bruk och att använda det oförändrat för ickekommersiell forskning och för undervisning. Överföring av upphovsrätten vid en senare tidpunkt kan inte upphäva detta tillstånd. All annan användning av dokumentet kräver upphovsmannens medgivande. För att garantera äktheten, säkerheten och tillgängligheten finns det lösningar av teknisk och administrativ art.

Upphovsmannens ideella rätt innefattar rätt att bli nämnd som upphovsman i den omfattning som god sed kräver vid användning av dokumentet på ovan beskrivna sätt samt skydd mot att dokumentet ändras eller presenteras i sådan form eller i sådant sammanhang som är kränkande för upphovsmannens litterära eller konstnärliga anseende eller egenart.

För ytterligare information om Linköping University Electronic Press se förlagets hemsida: `http://www.ep.liu.se/`

English

The publishers will keep this document online on the Internet - or its possible replacement - for a considerable time from the date of publication barring exceptional circumstances.

The online availability of the document implies a permanent permission for anyone to read, to download, to print out single copies for your own use and to use it unchanged for any non-commercial research and educational purpose. Subsequent transfers of copyright cannot revoke this permission. All other uses of the document are conditional on the consent of the copyright owner. The publisher has taken technical and administrative measures to assure authenticity, security and accessibility.

According to intellectual property law the author has the right to be mentioned when his/her work is accessed as described above and to be protected against infringement.

For additional information about the Linköping University Electronic Press and its procedures for publication and for assurance of document integrity, please refer to its WWW home page: `http://www.ep.liu.se/`

© Magnus Hellström
Linköping, 16th February 2005